

## Supplementary Information: Probing the Effect of Surface Strain on CO Binding to Pd Thin Films

Dan J. Harding,<sup>a,b,c,\*</sup> Marian David Bongers,<sup>d</sup> Stefan Wagner,<sup>e</sup> Hinrich Hahn,<sup>a,b</sup> Jannis Neugeboren,<sup>a,b</sup> T.N. Kitsopoulos,<sup>a,b,f,g</sup> Alec M. Wodtke,<sup>a,b,h</sup> and Astrid Pundt<sup>d,e</sup>

<sup>a</sup> Institut für Physikalische Chemie, Georg-August-Universität Göttingen, Göttingen, Germany.

<sup>b</sup> Max-Planck-Institut für biophysikalische Chemie, Göttingen, Germany.

<sup>c</sup> Dept. of Chemical Engineering, KTH Royal Institute of Technology, Teknikringen 42, 10044 Stockholm, Sweden.

<sup>d</sup> Institut für Materialphysik, Georg-August-Universität Göttingen, Göttingen, Germany.

<sup>e</sup> Institute of Applied Materials (IAM-WK), Karlsruhe Institute of Technology KIT, Engelbert-Arnold-Straße 4, 76131 Karlsruhe, Germany.

<sup>f</sup> Department of Chemistry, University of Crete, Heraklion, Greece.

<sup>g</sup> Institute of Electronic Structure and Laser, FORTH, Heraklion, Greece.

<sup>h</sup> International Center for Advanced Studies of Energy Conversion, Georg-August University of Göttingen, Göttingen, Germany.

\* [djha@kth.se](mailto:djha@kth.se) [orcid.org/0000-0002-8622-9046](https://orcid.org/0000-0002-8622-9046)

## 1 XRD Rocking Curve

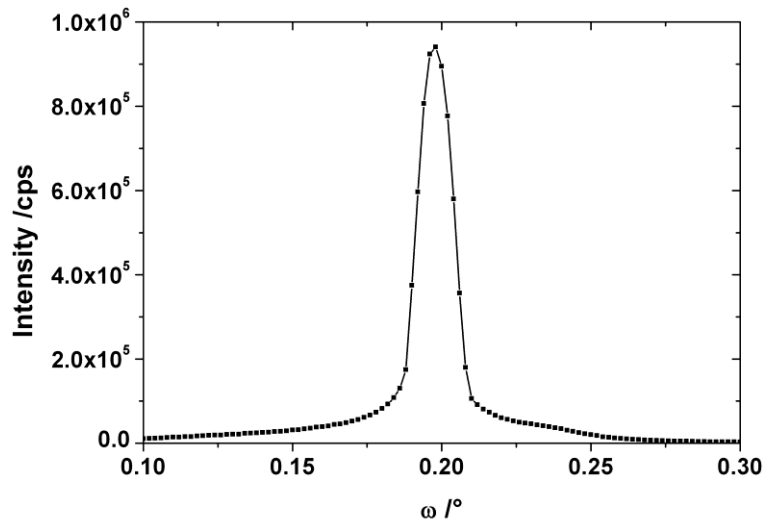
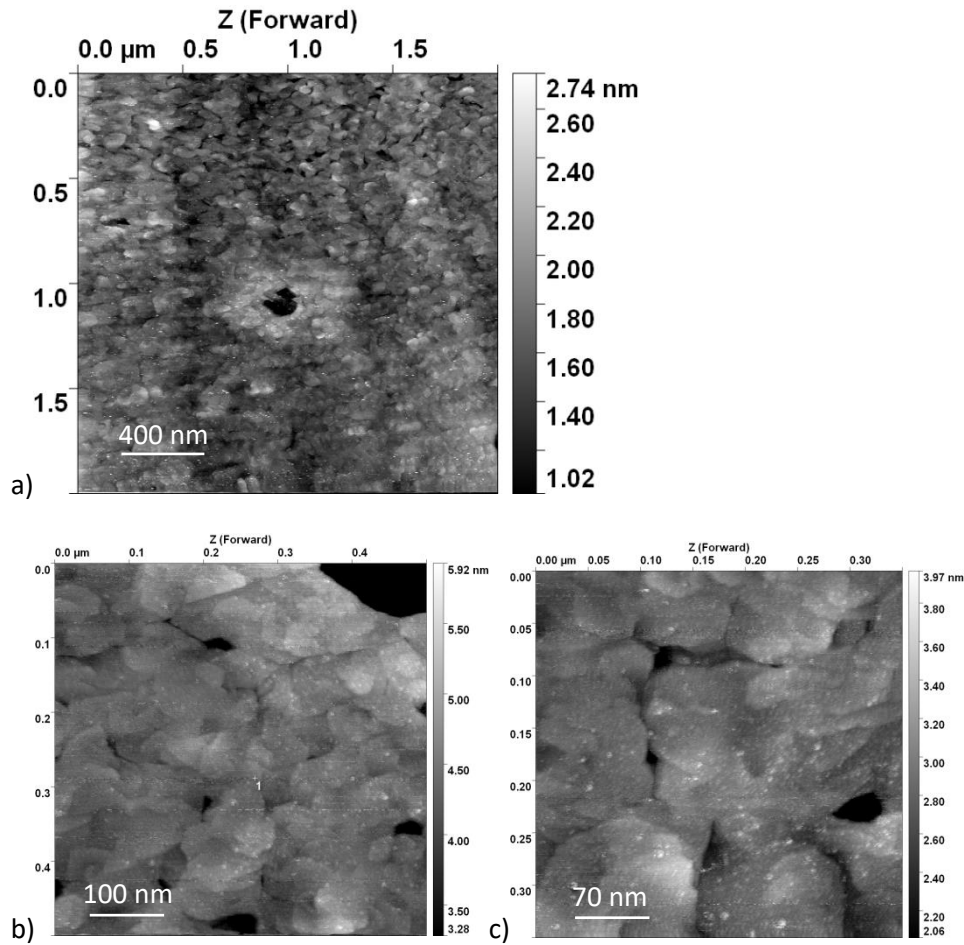


Figure S1: Rocking Curve for the 16 nm sample measured in total reflectance mode. The  $fwhm = 0.014^\circ \pm 0.001^\circ$  is consistent with a flat and homogeneous sample

## 2 Estimation of the grain boundary area by STM

STM topography measurements were performed on the 16 nm Pd(111) film. Figure S2 shows several STM images of the Pd film, with two different resolutions. Fig. S2 a) shows the surface topography, a substructure can be clearly seen. This is magnified in b) and c). The topography is not easy to interpret. Dislocations can be found on some places and possibly small angle grain boundaries. The latter is interpreted from the interfaces of the grain like structures. Further, some very small holes can be found that are up to 3 nm deeper in the Pd film.



**Figure S2: STM images in different magnification. a) 2 μm x 2 μm image revealing the terraces and substructure on the Pd film. b) and c) show magnifications of this structure.**

We have estimated the fraction of the surface made up of grain boundaries (GB) from STM images. Examples are shown in Fig. S2. We first identify and count the grains in the images. From the number of grains,  $N$ , and the area of the image,  $A_i$ , we determine the average grain area and, assuming the grains are circular, their radius,  $r_g$

$$\text{Ave. grain area} = \frac{A_i}{N} = \pi r_g^2$$

$$\text{Ave. grain radius} = r_g = \sqrt{\frac{A_i}{\pi N}}$$

For the 16 nm film we obtain a value of  $r_g = (36 \pm 5)$  nm. The fraction of GBs can then be determined for the average grain from the area of the boundary, i.e. the grain circumference times half the width of the GB,  $w_{gb} = 1$  nm, to the area of the grain

$$\text{GB fraction} = \frac{0.5 w_{gb} 2\pi r_g}{\pi r_g^2} = \frac{w_{gb}}{r_g} = 0.028 \pm 0.003$$

### 3 Thermal expansion of a thin Pd layer on a r-TiO<sub>2</sub>(110) crystal

The thin Pd layers exhibit an out-of-plane (111) crystal orientation on the r-TiO<sub>2</sub>(110) crystals. The strain in the Pd layer is temperature dependent and depends on the Pd bulk reference state at the same temperature. It is modified by the temperature dependent lattice mismatch of film and substrate.

In the linear elastic limit, bounds on the total mismatch strain of the Pd film are given as a function of temperature by

$$\varepsilon(T) = \frac{p \cdot d_{\text{TiO}_2}(T) - q \cdot d_{\text{Pd}}(T)}{q \cdot d_{\text{Pd}}(T_0)} - \frac{p \cdot d_{\text{TiO}_2}(T_0) - q \cdot d_{\text{Pd}}(T_0)}{q \cdot d_{\text{Pd}}(T_0)} - \varepsilon_0, \quad (\text{S1})$$

with the substrate's and the film's ideal in-plane lattice parameters  $d_{\text{TiO}_2}(T)$  and  $d_{\text{Pd}}(T)$  at the temperature of the VRK experiments,  $d_{\text{TiO}_2}(T_0)$  and  $d_{\text{Pd}}(T_0)$  in the reference state at  $T_0$ , the numbers  $p$  and  $q$  of the substrate's and the film's lattice planes matching at the interface, and the measured strain  $-\varepsilon_0$  at  $T_0$ . Thereby  $-\varepsilon_0$  can differ from the ideal strain at  $T_0$  due to stress relaxation of the film.

The ideal temperature-dependency of the film's and the substrate's lattice parameters can be calculated from the thermal expansion coefficients. As the films show increased epitaxy after heating, the orientation relationship has to be accounted for. Furthermore, the r-TiO<sub>2</sub> substrates' thermal expansion is strongly anisotropic. Therefore, the thermal strain of the film has to be treated anisotropically for the directions of the epitaxial relationship.

For the thin layers, the same orientation relationship as for the 200 nm Pd layers is assumed between the Pd layer and the r-TiO<sub>2</sub> crystal (see Ref. 1, chap. 2.3.1):

Pd[ $\bar{2}11$ ]||r-TiO<sub>2</sub>[ $\bar{1}10$ ] ("a-direction")

and

Pd[ $0\bar{1}1$ ]||r-TiO<sub>2</sub>[001] ("c-direction").

Owing to Poissons effect, then the film stresses follow according to Ref. 2

$$\sigma_a(T) = \frac{E}{1-\nu^2} [\varepsilon_a(T) + \nu \cdot \varepsilon_c(T)] \quad (\text{S2})$$

and

$$\sigma_c(T) = \frac{E}{1-\nu^2} [\varepsilon_c(T) + \nu \cdot \varepsilon_a(T)] \quad (S3)$$

in  $a$ - and  $c$ -direction, respectively, with  $E = 136.1$  GPa and  $\nu = 0.523$  of the Pd film in directions perpendicular to the  $[111]$  direction.<sup>2</sup>

At room temperature, ideal lattice parameters of  $r$ -TiO<sub>2</sub> and Pd in the desired directions are given in table S1.

$a$ -direction (293 K)		$c$ -direction (293 K)	
TiO <sub>2</sub> $[\bar{1}10]$	Pd $[\bar{2}11]$	TiO <sub>2</sub> $[001]$	Pd $[0\bar{1}1]$
$3.24717 \pm 0.00022$ Å	$1.58816 \pm 0.00026$ Å	$2.95734 \pm 0.00027$ Å	$2.75078 \pm 0.00045$ Å
$p = 14$	$q = 29$	$p = 27$	$q = 29$

*Table S1: Ideal lattice parameters of  $r$ -TiO<sub>2</sub> substrate and Pd film in  $a$ - and  $c$ -direction at  $T = 293$  K, and resulting ideal lattice matching parameters  $p$  and  $q$ , see eq. (S1).*

The minimum lattice misfit follows for  $p = 14$  and  $q = 29$  for  $a$ -direction, and for  $p = 27$  and  $q = 29$  for  $c$ -direction.

For the case of the  $a$ -direction we have investigated the film-substrate interface of a 200 nm Pd film deposited by magnetron sputtering at 1023 K with HRTEM. As shown in figure S3, experimentally determined values of  $p = 15$  and  $q = 21$  are present. We ascribe this difference from the theoretically expected to the observed  $p$ - and  $q$ -values to stress relaxation in the Pd film by the implementation of misfit dislocations at the interface. As the lattice parameters in eq. S1 are calculated for the ideal linear elastic case and we consider elastic bounds of the films' thermal expansion, we will use the theoretical  $p$ - and  $q$ -values in our subsequent strain and stress calculations.

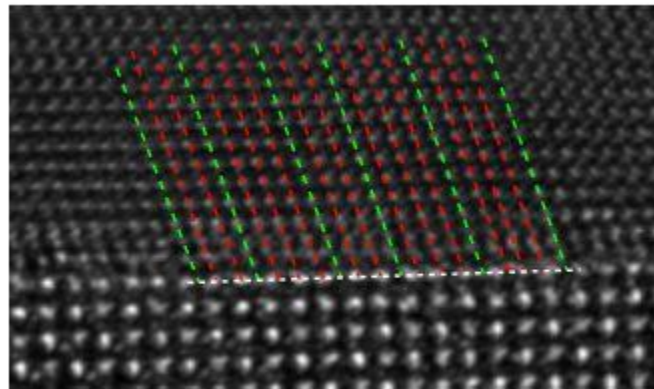


*Figure S3: HRTEM image of the Pd $[111]$ / $r$ -TiO<sub>2</sub> $[110]$  interface of a 200 nm Pd film [1], imaged with an FEI Titan 80-300 ETEM with Cs-image corrector at 300 keV. The Pd $[\bar{2}11]$  and the TiO<sub>2</sub> $[\bar{1}10]$  direction are parallel and pointing to the right. Indicated in green are misfit dislocations which are incorporated to*

reduce the stress state of the Pd film and with red those Pd( $\bar{1}11$ ) planes which fit on TiO<sub>2</sub>(110) planes. Here,  $q = 21$  Pd( $\bar{1}11$ ) planes match to  $p = 15$  TiO<sub>2</sub>(110) planes. Reprinted with permission from Ref. 1, copyright 2018.

The calculated temperature dependencies of the 16 nm film's strains (eq. S1) are given in figure S2. The temperature range of the VRK experiments is marked by the shaded region. Thereby, the strains have been centered around the experimentally determined  $-\varepsilon_0 = 0.0029$ , see main text. As XRD yields out-of-plane strains referring to the sum of the in-plane strains in case of films with [111] texture, we have assumed isotropic in-plane strains  $\varepsilon_{11} = \varepsilon_{22} = -\varepsilon_0$ , for simplicity. It is<sup>3</sup>

$$\varepsilon_{33} = -\frac{C_{11}+2C_{12}-2C_{44}}{C_{11}+2C_{12}+4C_{44}}(\varepsilon_{11} + \varepsilon_{22}) \quad (S4)$$

for [111] textured films, yielding

$$-2 \cdot \varepsilon_{33} \approx \varepsilon_{11} + \varepsilon_{22} \quad (S5)$$

for the case of Pd films with the elastic compliances  $C_{11} = 224$  GPa,  $C_{12} = 173$  GPa and  $C_{44} = 71.6$  GPa [4].

The corresponding in-plane stresses, referring to eq. (S2) and (S3), are given in figure S3.

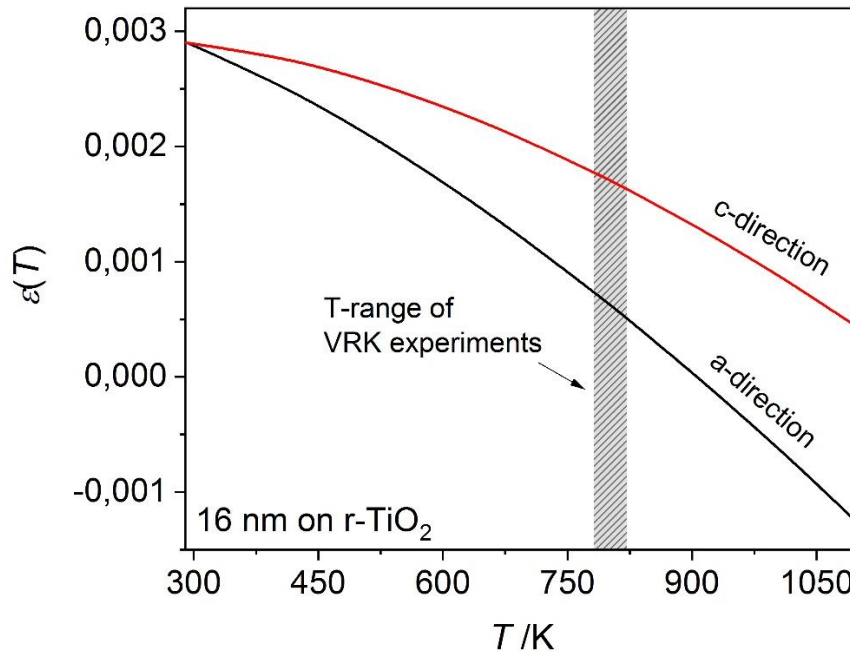


Figure S4: In-plane strains of 16 nm Pd on r-TiO<sub>2</sub> in a- and c-directions as a function of temperature. The offset  $-\varepsilon_0 = 0.0029$  at  $T = 293$  K was determined by XRD. The T-range of the VRK experiments is marked by the shaded region.

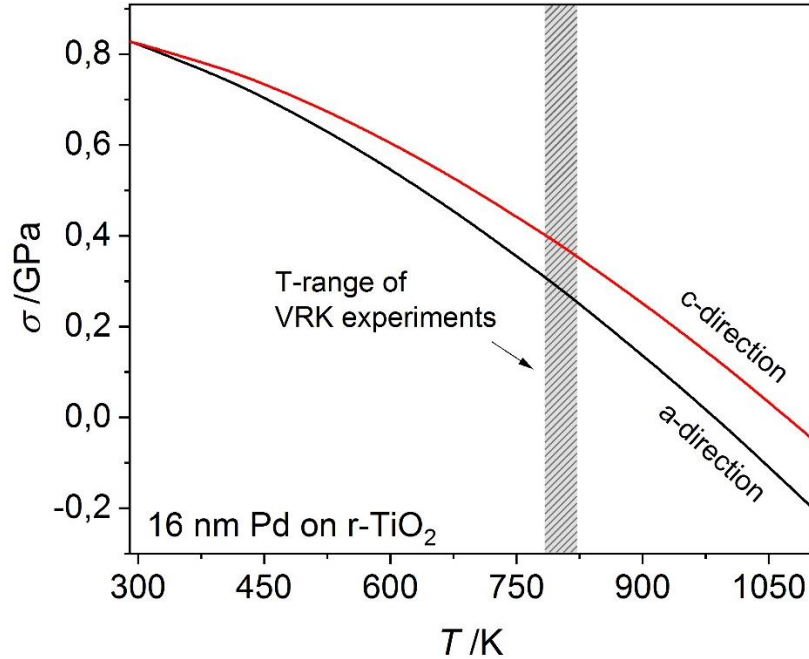


Figure S5: In-plane stresses of 16 nm Pd on r-TiO<sub>2</sub> as a function of temperature in a- and c-directions. The stresses are calculated by eq. S2 and S3 from the corresponding strains which are shown in figure S2. The temperature range of the VRK experiments is marked by the shaded region.

Therefore, the 16 nm film was subject to tensile stress on the order of  $\sigma_a = 0.28$  GPa and  $\sigma_c = 0.38$  GPa at  $T_{VRK} = 803$  K during the VRK experiments. The resulting stress anisotropy is small. The corresponding in-plane strains, that are controlling the binding energy of the Pd film surface, reveal a larger anisotropy with  $\varepsilon_a = 0.0006$  and  $\varepsilon_c = 0.0017$  at  $T_{VRK} = 803$  K.

The tensile stress of the Pd film at elevated temperatures is reduced in comparison to room temperature, as a metal film, in general, expands more with temperature than a ceramic substrate. The substrate induced strain thereby implies a compressive stress contribution to the film.

Pd film thickness /nm	T /K	$\varepsilon_a$ /%	$\varepsilon_c$ /%	$\sigma_a$ /GPa	$\sigma_c$ /GPa
16.4	293	$0.29 \pm 0.04$	$0.29 \pm 0.04$	$0.83 \pm 0.08$	$0.83 \pm 0.08$
	783	$0.07 \pm 0.04$	$0.18 \pm 0.04$	$0.31 \pm 0.08$	$0.40 \pm 0.08$
	803	$0.06 \pm 0.04$	$0.17 \pm 0.04$	$0.28 \pm 0.08$	$0.38 \pm 0.08$
	823	$0.05 \pm 0.04$	$0.16 \pm 0.04$	$0.25 \pm 0.08$	$0.35 \pm 0.08$

Table S2: In-plane strains  $\varepsilon$  and corresponding in-plane stresses  $\sigma$  of the investigated Pd thin films on r-TiO<sub>2</sub> at different temperatures during XRD measurements and VRK experiments. The error values were calculated according to Gaussian error propagation.

## 4 Thermal expansion

### 4.1 Rutile titanium dioxide

The temperature dependent in-plane lattice parameters  $d_a(T)$  and  $d_c(T)$  of r-TiO<sub>2</sub> were calculated referring to the crystal structure investigations of rutile performed by Sugiyama et al.<sup>5</sup> There, the anisotropic linear expansion coefficients  $\alpha$  in  $a$ - and  $c$ - direction are given up to 1873 K.

It is<sup>5</sup>

$$\alpha_a = 8.9(1) \cdot 10^{-6}/^{\circ}C \quad (S6)$$

and

$$\alpha_c = 11.1(1) \cdot 10^{-6}/^{\circ}C \quad (S7)$$

According to the definition of the linear expansion coefficient the corresponding lattice parameters in  $a$ - and  $c$ -direction follow with

$$d_{(hkl)}(T) = \left(1 + \alpha_{(hkl)} \cdot (T - T_0)\right) \cdot d_{(hkl)}(T_0) \quad (S8)$$

with  $d_{(\bar{1}10)}(T_0) \equiv d_a(T_0) = 3.2473 \pm 0.0002 \text{ \AA}$  and  $d_{(001)}(T_0) \equiv d_c(T_0) = 2.9575 \pm 0.0002 \text{ \AA}$  at  $T_0 = 25 \text{ }^{\circ}C$  (298 K), compare [5], and the corresponding expansion coefficient  $\alpha_{(hkl)}$ .

### 4.2 Palladium

The temperature dependent lattice parameter  $a(T)$  of Pd is given in  $\text{\AA}$  from Arblaster<sup>6</sup> with

$$a(T) = \left(1 + \frac{\delta a(T)}{a(T_0)}\right) \cdot a(T_0) \quad (S9)$$

where  $\frac{\delta a(T)}{a(T_0)}$  is the thermal expansion equation

$$\frac{\delta a(T)}{a(T_0)} = -3.67831 \cdot 10^{-3} + 1.10122 \cdot 10^{-5} \cdot T + 2.69121 \cdot 10^{-9} \cdot T^2 - 2.25680 \cdot 10^{-13} \cdot T^3 + \frac{6.58134 \cdot 10^{-2}}{T} \quad (S10)$$

at  $T_0 = 293 \text{ K}$ . Thereby  $a(T_0) = 3.89018 \pm 0.0006 \text{ \AA}$ .

It follows

$$d_{(uvw)}(T) = \frac{1}{\sqrt{u^2 + v^2 + w^2}} \cdot a(T) \quad (S11)$$

with  $(uvw) = (\bar{2}11)$  or  $(1\bar{1}0)$  for  $a$ - and  $c$ -direction, respectively.

## References

- [1] Bongers, M. D. In situ Studies on Palladium/Rutile Titanium Dioxide Exposed to Low Pressure Hydrogen Gas Environments. Ph.D. Thesis, Georg-August-Universität Göttingen: Niedersächsische Staats- und Universitätsbibliothek Göttingen, **2018**.
- [2] Wagner, S. Dünne Palladium-Wasserstoff-Schichten als Modellsystem: Thermodynamik Struktureller Phasenübergänge Unter Elastischen und Mikrostrukturellen Zwangsbedingungen, Ph.D. Thesis, Georg-August-Universität Göttingen: Niedersächsische Staats- und Universitätsbibliothek Göttingen, **2014**.
- [3] Sander, D. The Correlation Between Mechanical Stress and Magnetic Anisotropy in Ultrathin Films. *Rep. Prog. Phys.* **1999**, *62*, 809-858.
- [4] Pundt, A. Nanoskalige Metall-Wasserstoff-Systeme, Ph.D. Thesis, Georg-August-Universität Göttingen: Niedersächsische Staats- und Universitätsbibliothek Göttingen, **2005**.
- [5] Sugiyama, K.; Takeuchi, Y. The Crystal Structure of Rutile as a Function of Temperature up to 1600 °C. *Z. f. Krist.* **1991**, *194*, 305-313.
- [6] Arblaster, J. W. Crystallographic Properties of Palladium. *Platin. Met. Rev.* **2012**, *56*, 181-189.